

# Influence of the Small-Scale Magnetic Field on the Evolution of the Angle between the Magnetic Moment and Rotation Axis of Radio Pulsars with Superfluid Cores

D. P. Barsukov<sup>1,2</sup>, O. A. Goglichidze<sup>1</sup>, and A. I. Tsygan<sup>1\*</sup>

<sup>1</sup>*Ioffe Physical–Technical Institute, Russian Academy of Sciences,  
ul. Politekhnikeskaya 26, St. Petersburg, 194021 Russia*

<sup>2</sup>*St. Petersburg State Technical University,  
ul. Politekhnikeskaya 29, St. Petersburg, 195251 Russia*

Received January 17, 2012; in final form, June 6, 2012

**Abstract**—The evolution of the angle between the magnetic moment and rotation axis of radio pulsars (inclination angle) is considered taking into account the presence of a non-dipolar magnetic field at the neutron-star surface and superfluid neutrons in the stellar interior. It is assumed that the total loss of angular momentum by the pulsar can be represented as a sum of magnetodipole and current losses. The neutron star is treated as a two-component system consisting of a charged component (including protons and electrons, as well as the crust, which is rigidly coupled with them, and normal neutrons) and a superfluid core. The components interact through scattering of degenerate electrons on magnetized Feynman–Onsager vortices. If a superfluid core is absent, then, in spite of the presence of stable equilibrium inclination angles, the rate with which these are reached is so slow that most pulsars do not have sufficient time to approach them during their lifetimes. The presence of superfluid neutrons results, first, in faster evolution of the inclination angle and, second, in the final stage of the evolution being either an orthogonal or a coaxial state. The proposed model fits the observations better in the case of small superfluid cores.

DOI: 10.1134/S1063772913010022

## 1. INTRODUCTION

The number of radio pulsars for which the angle between the magnetic and rotation axes (inclination angle) can be measured is constantly growing (see, e.g., [1]). However, the evolution of this tilt is a complex problem theoretically, which currently has no obvious solution. On the one hand, this is related to the structure of the neutron-star magnetosphere, which determines the loss of angular momentum by the pulsar. On the other hand, it is related to the internal structures of neutron stars (angular momentum redistribution between the crust, where the magnetic field is frozen, and deeper layers).

Recently, more theoretical and observational evidence has been accumulated suggesting that the magnetic fields near the surfaces of neutron stars can differ considerably from a dipolar field whose value is determined by the pulsar spin-down. In addition to the large-scale dipolar magnetic field, there are probably also small-scale magnetic fields that rapidly decrease with distance from the star. Obviously, if the intensity of the small-scale fields does not exceed

the intensity of the dipolar field by two to three orders of magnitude at the stellar surface, the contribution of these fields to the total magnetic field will be negligible near the light cylinder. Thus, if the pulsar's angular-momentum losses are determined solely by the magnetodipole mechanism, the presence of small-scale fields has no effect on these losses.

However, the presence of magnetic anomalies near the magnetic poles of the star should result in bending of the pulsar tubes (regions of open field lines), which, in turn, can influence the electric current in the inner gap, and consequently the loss of angular momentum, which is carried away by particles along the open field lines. This means that the presence of small-scale magnetic fields can have an important effect on the spin-down and evolution of the inclination angles of pulsars.

## 2. TORQUE ACTING ON A STAR

There are two main mechanisms for angular-momentum losses for neutron stars: magnetodipole and current. The first is related to magnetodipole radiation of the rotating magnetized neutron star [2]. The calculation of the torque due to the radiative

\*E-mail: [tsygan@astro.ioffe.ru](mailto:tsygan@astro.ioffe.ru)

reaction requires knowledge of the structure of the magnetosphere. However, this is an independent theoretical problem, which, generally speaking, currently has no unambiguous solution (see, e.g., [3]). In this paper, we use the torque acting on a magnetized conductive sphere rotating in vacuum:

$$\vec{K}_{dip} = K_0 (\vec{e}_m \cos \chi - \vec{e}_\Omega + R[\vec{e}_\Omega \times \vec{e}_m]). \quad (1)$$

Here,  $\chi$  is the inclination angle,  $\vec{\Omega} = \Omega \vec{e}_\Omega$ ,  $\vec{m} = m \vec{e}_m$ ,  $\vec{\Omega}$  is the angular-velocity vector of the neutron star, and  $\vec{m}$  is its magnetic moment. This torque was first used in application to a neutron star in [4] (see also [5]). In the limit of small angular velocities,  $\Omega r_{ns}/c \ll 1$ , the factors  $K_0$  and  $R$  are

$$K_0 = \frac{2}{3} \frac{m^2 \Omega^3}{c^3}, \quad (2)$$

$$R = \frac{3}{2} \delta \left( \frac{c}{\Omega r_{ns}} \right) \cos \chi, \quad (3)$$

where  $\delta \sim 1$  is a factor depending on the configuration of the surface currents. Here, we adopted  $\delta = 3/5$ , which corresponds to an absence of surface currents [5].

The second mechanism is related to electric currents flowing along pulsar tubes. Since charges of the same sign should escape along both tubes, for the star to preserve its electrical neutrality, there must be return currents in the magnetosphere that compensate the loss of charge from the neutron star. The most natural location for such currents are the equipotential walls of the pulsar tubes. Thus, the electric currents should close under the surface of the pulsar caps. Since the currents flow across the magnetic-field lines there, they are subject to a Lorentz force resulting in the spin-down of the star. The torque corresponding to this mechanism can be represented [6]

$$\vec{K}_{cur} = -K_0 \alpha \cos \chi \vec{e}_m. \quad (4)$$

We have introduced the parameter  $\alpha$  here, which can be expressed in terms of the current density in the tubes [7]:

$$\alpha = \frac{3}{4} \frac{j_N + j_S}{j_{GJ}}, \quad (5)$$

where  $j_{N(S)}$  are the current densities in the northern and southern tubes, respectively,  $j_{GJ} = (\Omega B_0 / 2\pi) \cos \chi$ , and  $B_0$  is the magnetic field at the magnetic poles of the star.

Following Jones [6], we assume that the total torque acting on the neutron star is the sum of (1) and (4) (see also [8]):

$$\vec{K} = \vec{K}_{dip} + \vec{K}_{cur}. \quad (6)$$

This assumption can be justified as follows. The magnetodipole and current losses are related to the momentum flux associated with a small deviation of the stellar magnetic field from a dipolar field. Thus, while the magnetodipole mechanism, generally speaking, creates an energy flux in all directions, the momentum flux related to the current losses exists only inside the pulsar flux tubes (see, e.g., [9]). Thus, the momentum fluxes related to different types of losses intersect only inside these tubes. Here, the perturbations of the field due to current losses substantially exceed those due to magnetodipole losses. This means that these latter losses can be neglected inside the tubes; in view of the small angular size of the tubes, this will not result in a large error.

### 3. SMALL-SCALE MAGNETIC FIELD

Let us now take into account bending of the pulsar tubes due to the presence of small-scale fields near the magnetic poles of the star. It is believed that, in the first several tens of seconds of its life, a neutron star is subject to various hydromagnetic instabilities, which lead to the generation of its dipolar field via the dynamo mechanism. After the completion of the convective stage, the magnetic field is frozen into the crystallizing crust of the neutron star, and the subsequent evolution of the field is connected with the dissipation of the electric currents maintaining the field. Calculations demonstrate (see, e.g., [10]) that the size of the largest convective cells is of the order of 1 km ( $\sim 0.1 r_{ns}$ ). Fields on such scales are generated most efficiently in the convective stage. Furthermore, such fields decay more slowly than smaller-scale fields [11]. Thus, the magnetic fields of neutron stars probably corresponds to a superposition of a large-scale dipole field and a small-scale field in which harmonics with  $l \sim 20$  dominate.

Further, we note that bending of the pulsar tubes is mainly determined by the horizontal component of the small-scale magnetic field (at least if it does not appreciably exceed the intensity of the dipole field at the stellar surface). A simple way of modeling small-scale fields near the magnetic poles taking into account the above remarks was proposed in [12]. An additional magnetic dipole  $\vec{m}_1$  oriented perpendicular to the main dipole  $\vec{m}$  (Fig. 1) is placed at depth  $\Delta \cdot r_{ns}$  on the magnetic axis of the star.

Let us introduce an orthonormal coordinate basis  $(\vec{e}_x, \vec{e}_y, \vec{e}_z)$  corotating with the star:

$$\dot{\vec{e}}_i = [\vec{\Omega} \times \vec{e}_i], \quad i = x, y, z, \quad \vec{e}_z = \vec{e}_m. \quad (7)$$

The expression for  $\vec{m}_1$  can then be written

$$\vec{m}_1 = 2m\nu \Delta^3 (\vec{e}_x \cos \gamma + \vec{e}_y \sin \gamma). \quad (8)$$

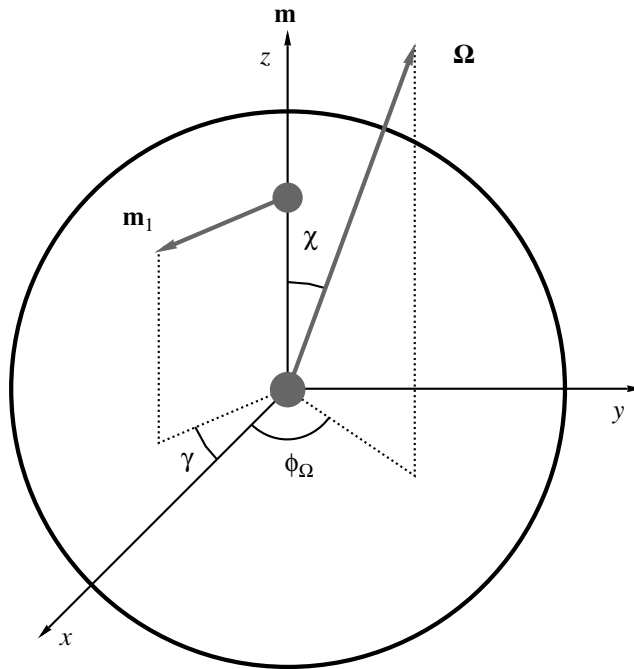


Fig. 1. Vectors and angles used, specifying their positional relationships.

Here,  $\nu = B_0/B_1$  is the non-dipolarity parameter,  $B_0$  and  $B_1$  are the fields created by the main dipole and the additional magnetic dipole on the  $z$  axis at point  $r = r_{ns}$ , and the angle  $\gamma$  determines the orientation of the vector  $\vec{m}_1$  in the plane determined by the vectors  $(\vec{e}_x, \vec{e}_y)$ . We consider here the case  $\nu \lesssim 1$ . We assumed  $\Delta = 0.1$ , which ensures coincidence of the vertical scale height for the variation of the horizontal component of the magnetic field and the similar characteristic scale for the variation of the multipolar harmonics with  $l \sim 20$  near the stellar surface.

Using the coordinate basis (7), we introduce the spherical coordinates  $(\eta = r/r_{ns}, \theta, \phi)$ . Then, neglecting the curvature of space near the surface of the neutron star, we can write the components of the total magnetic field in the small-angle approximation ( $\theta \ll 1$ )

$$\begin{cases} B_r = \frac{B_0}{\eta^3}, \\ B_\theta = -\frac{B_0}{\eta^3} \mu(\eta) \cos(\phi - \gamma), \\ B_\phi = \frac{B_0}{\eta^3} \mu(\eta) \sin(\phi - \gamma), \end{cases} \quad (9)$$

where we have introduced

$$\mu(\eta) = \nu \left( \frac{\Delta \eta}{\eta - 1 + \Delta} \right)^3. \quad (10)$$

If the pulsar is not too close to the orthogonal state and the pulsar tube is sufficiently thin, the Goldreich–Julian density inside the tube not too far from the

stellar surface ( $\eta \ll (c/\Omega r_{ns}) \cot \chi$ ) can be written [9, 13]

$$\rho_{GJ} \approx -\frac{\Omega B(\eta)}{2\pi c} f_\nu(\eta, \chi, \varphi_\Omega) \cos \chi, \quad (11)$$

where we have neglected terms of order  $\theta_0 \sqrt{\eta} \sin \chi$ . In addition,  $B(\eta)$  is the total magnetic field here. The function  $f_\nu(\eta, \chi, \varphi_\Omega)$  has the form:

$$f_\nu(\eta, \chi, \varphi_\Omega) = \frac{1}{\sqrt{1 + \mu^2(\eta)}} \left[ \left( 1 - \frac{\varkappa}{\eta^3} \right) + \mu(\eta) \left( 1 + \frac{\varkappa}{2\eta^3} \right) \tan \chi \cos(\varphi_\Omega - \gamma) \right]. \quad (12)$$

The angles  $\chi$ ,  $\varphi_\Omega$ , and  $\gamma$  determine the mutual orientation of the vectors  $\vec{m}$ ,  $\vec{m}_1$ , and  $\vec{\Omega}$  (Fig. 1). The factor  $\varkappa$  describes the effect of frame dragging [14]. For a typical neutron star,  $\varkappa \approx 0.15$ . Note that, when  $\varkappa = 0$ , the function  $f_\nu(\eta, \chi, \varphi_\Omega)$  coincides with the cosine of the angle between  $\vec{B}$  and  $\vec{\Omega}$ .

We used the electrodynamic model [9] for a pulsar tube bent in this way. We first assumed for concreteness that  $\cos \chi > 0$ . We also assumed that the surface of the polar caps was able to emit particles in a space charge limited flow regime ( $E_{||} = (\vec{E} \cdot \vec{B})/B = 0$  for  $\eta = 1$ ). Calculations demonstrate that electrons should always escape freely from the polar caps of neutron stars. However, generally speaking, for sufficiently strong magnetic fields and not very high

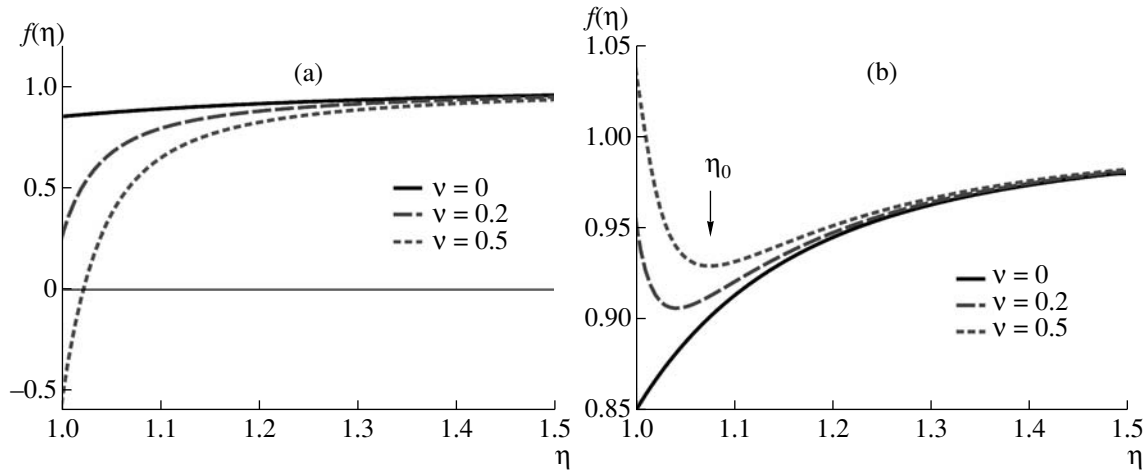


**Fig. 2.** Behavior of the function  $f_\nu(\eta, \chi, \varphi_\Omega)$  for various non-dipolarity parameters  $\nu$ : (a) for the case  $\cos(\varphi_\Omega - \gamma) < 0$ , (b) for the case  $\cos(\varphi_\Omega - \gamma) > 0$ .

surface temperatures, this statement may not be valid for protons (see, e.g., [15]). This circumstance limits the applicability of the model proposed here for the case  $\cos \chi < 0$ .

Note that, since the density  $\rho_{GJ}$  can be either non-monotonic along the magnetic-field lines or change sign along these lines for some orientations of the tube relative to the stellar rotation axis, a stable (stationary) region of particle acceleration (pulsar diode) can exist in curved tubes, which is, generally speaking, not always right at the neutron-star surface. However, it is supposed that a monotonic decrease of the negative Goldreich–Julian density is a sufficient condition for the existence of a stable pulsar diode in some region of the tube. This means that the electric potential increases monotonically along the field lines in this region. It can be shown that this is true in two limiting cases: in a flat tube [16] and in a long thin tube [13]. The main assumption of the model [9] is that the pulsar diode is at the minimum possible height. Thus, study of the operational mode of the pulsar tube reduces to study of the behavior of the density  $\rho_{GJ}$ , which, in turn, reduces to study of the behavior of the function  $f_\nu(\eta, \chi, \varphi_\Omega)$ .

It can be shown that, in the case of a space charge limited flow regime, the current density in the tube is approximately

$$j(\eta) \approx c\rho_{GJ}(\eta_0) \frac{B(\eta)}{B(\eta_0)}, \quad (13)$$

where  $\eta_0$  is the position of the cathode of the pulsar diode.

Let us consider possible cases in more detail. First, let  $\cos(\varphi_\Omega - \gamma) < 0$ . Then, the function  $f_\nu(\eta, \chi, \varphi_\Omega)$  increases monotonically with altitude. If  $\nu \tan \chi$  is not very large, then  $f_\nu(1, \chi, \varphi_\Omega) > 0$ .

It is then natural to suppose that, as in the case of a dipole field, the diode is right at the surface of the star. In this case,  $\eta_0 = 1$ , and expression (13) is valid. However, if  $\nu \tan \chi$  begins to exceed  $(1 - \kappa)(1 + \kappa/2)^{-1} |\cos \varphi_\Omega|^{-1}$ , the value of  $f_\nu(\eta, \chi, \varphi_\Omega)$  for  $\eta = 1$  becomes negative and reaches zero at some point  $\eta_0 > 1$  (Fig. 2a). In this case, it would seem that the pulsar diode cannot be at the stellar surface. The minimum possible height is at  $\eta_0$ . The region of the tube from the surface to  $\eta_0$  should be filled with positively charged particles, which, due to the force of gravity acting on them, create a potential barrier for electrons. In this case, the current in the tube is extremely small. Let us suppose that it is zero in this configuration ( $j = 0$ ). Since the function  $f_\nu(1, \chi, \varphi_\Omega)$  also vanishes at  $\eta_0$ , formula (13) is formally applicable here as well.

If  $\cos(\varphi_\Omega - \gamma) > 0$ , the function  $f_\nu(\eta, \chi, \varphi_\Omega)$  is always positive. However, for sufficiently large values of  $\nu \tan \chi$ , it becomes non-monotonic (Fig. 2b). In this case, it is supposed that the diode begins at  $\eta_m$ , which determines the minimum of  $f_\nu(\eta, \chi, \varphi_\Omega)$ . Below this point, there should probably be oscillations of the potential similar to those obtained in [17]. In this case, the current is again determined by (13), where in this case  $\eta_0 = \eta_m$ . Furthermore, for inclination angles  $\chi$  close to  $90^\circ$ , it is possible for  $f_\nu(\eta, \chi, \varphi_\Omega)$  to decrease to at least  $\eta = 5$ . In this case, we assumed that an outer gap is realized in the pulsar tube [18], so that the total current through it is zero.

#### 4. INTERNAL STRUCTURE OF NEUTRON STARS

As it was demonstrated in numerous papers dedicated to glitches, the internal structure of neutron

stars can have an important effect on the dynamics of their rotation. This concerns primarily the superfluid neutron component of the core. Superfluid neutrons interact weakly with the remaining material of the neutron star. The dominant mechanism for this interaction is scattering of degenerate electrons of the core on Feynman–Onsager vortices of the rotating superfluid liquid. The dynamic relaxation timescale for the velocity difference between the superfluid neutrons and electrons is considerably longer than the dynamic timescales describing the interaction of the remaining components of the core. Therefore, we can assume that protons, electrons, and normal neutrons represent one charged component of the core interacting with its superfluid neutron component.

Essentially, the interaction of electrons with vortex lines can be based on the following physical processes.

1. Scattering of electrons on excitations in vortex cores. This mechanism was studied in [19]. The calculations of [19] demonstrate that the relaxation timescale in this case is from several hours to essentially infinity. The efficiency of this mechanism is very sensitive to the temperature of the neutron-star core.

2. In cores of neutron stars,  ${}^3P_2$ -superfluidity is realized. This means that Cooper pairs have spins equal to unity and, accordingly, have magnetic moments that, in turn, result in magnetization of the vortex-line cores. Scattering of electrons on the magnetic field related to this magnetization was studied in [20]. The relaxation timescale obtained in [20] is about several years.

3. If in the neutron star the core protons are in a superconducting state, the proton fluid is entrained by vortical flows of the neutron fluid, and a magnetic field that substantially exceeds the field associated with the magnetization is generated along the lines. This mechanism was studied in [21]. It was shown that the relaxation timescale is

$$\tau_v = qP, \quad (14)$$

where  $P$  is the pulsar period and  $q = 10\text{--}200$  (this is determined by the effective mass of protons).

Thus, the third mechanism is the most efficient, and we assumed that the interaction between the components comes about via this mechanism. Note that, if the proton fluid is in a superconducting state of the second kind, Abrikosov vortices exist in this fluid, each of which carries the magnetic-flux quanta. However, we assumed that either the core protons are in a superconducting state of the first kind (the question of the type of superconductivity occurring is still under discussion; see, e.g., [22]) or the Abrikosov vortices interact only weakly with the vortex lines of the neutron fluid. The strong coupling of the proton and neutron vortices would result in a very fast

precession of the neutron star, in contradiction with observations (see, e.g., [23]).

The interaction of the neutron-star crust with the charged component of the core was studied in [24]. It was shown that the crust can essentially be considered to be rigidly bound to the charged component. Thus, treating a neutron star like a two-component system consisting of a charged component (including the core protons and electrons together with the crust and normal neutrons, which are rigidly bound to them) and of a superfluid component consisting of the core superfluid neutrons is quite justified.

Let us assume that the superfluid neutron core undergoes rigid-body rotation at the angular velocity  $\vec{\omega}$ . This means that the velocity field is

$$\vec{v}_s = [\vec{\omega} \times \vec{r}], \quad (15)$$

which, in turn, means that all vortex lines are parallel, aligned with  $\vec{\omega}$ , and distributed uniformly over the core volume. The density of vortex lines and  $\omega$  are related as

$$n_v \kappa = 2\omega, \quad (16)$$

where  $n_v$  is the number of vortex lines per unit area,  $\kappa = h/2m_n$  is the circulation quantum,  $h$  is the Planck constant, and  $m_n$  is the neutron mass.

For Feynman–Onsager vortices, the Magnus equation is valid (see, e.g., [25]):

$$\vec{F} = -\rho_n \vec{\kappa} \times (\vec{v}_l - \vec{v}_s), \quad (17)$$

where  $\vec{F}$  is the force per unit length of a vortex line,  $\vec{v}_l$  its velocity,  $\rho_s$  the mass density of the superfluid liquid, and  $\vec{\kappa}$  a vector numerically equal to the circulation quantum  $\kappa$  and aligned with  $\vec{\omega}$ .

Let the force  $\vec{F}$  acting on unit length of a vortex line from the charged component of the core be

$$\vec{F} = -C(\vec{v}_l - \vec{v}_c), \quad (18)$$

where  $\vec{v}_c$  is the velocity of the charged component of the core.

Substituting (18), (16), and (15) into (17) and taking into account that  $\vec{v}_c = [\vec{\Omega} \times \vec{r}]$ , we obtain after elimination of  $\vec{v}_l$

$$\begin{aligned} \vec{F} = & \rho_s k \frac{\sigma^2}{1 + \sigma^2} [\vec{e}_k \times [\vec{\mu} \times \vec{r}]] \\ & + \rho_s k \frac{\sigma}{1 + \sigma^2} [\vec{e}_k \times [\vec{e}_k \times [\vec{\mu} \times \vec{r}]]]. \end{aligned} \quad (19)$$

Here,  $\vec{\kappa} = \kappa \vec{e}_k$ ,  $\vec{\mu} = \vec{\Omega} - \vec{\omega}$ ,  $\sigma = C/\rho_s \kappa$ .

If (as we assumed) the force  $\vec{F}$  is related to the scattering of electrons on the magnetic field of the vortices, the factor  $C$  can be represented  $C = \rho_c/n_v \tau_v$  (see, e.g., [25]), where  $\rho_c$  is the mass density of the charged component of the core and  $\tau_v$  is the relaxation

timescale for the velocity calculated using (14). It is easy to check that, in this case,

$$\sigma = \frac{y}{4\pi q}, \quad (20)$$

where  $y = \rho_c/\rho_s$ . Note that  $\sigma \ll 1$ . In this situation, it is said that the components are weakly coupled.

The torque exerted by the charged component of the core on the superfluid component can be calculated as

$$\vec{N} = \int n_v [\vec{r} \times \vec{F}] dV. \quad (21)$$

The integral is taken over the volume of the superfluid core. Assuming  $\sigma$  to be constant and the superfluid core to be spherical, we obtain

$$\vec{N} = -\mathfrak{B}'[\vec{\omega} \times \vec{\mu}] + \mathfrak{B}\vec{e}_k(\vec{\omega} \cdot \vec{\mu}) + \mathfrak{B}\omega\vec{\mu}, \quad (22)$$

$$\mathfrak{B} \approx \sigma I_s, \quad \mathfrak{B}' \approx \sigma^2 I_s, \quad (23)$$

where  $I_s$  is the moment of inertia of the superfluid component of the core.

## 5. EQUATION OF MOTION

Let us write a set of equations of motion for the neutron-star components in the frame of reference corotating with the charged component:

$$\dot{\vec{M}}_c = \vec{K} - \vec{N}, \quad (24)$$

$$\dot{\vec{M}}_s = [\vec{M}_s \times \vec{\Omega}] + \vec{N}. \quad (25)$$

Here,  $\vec{M}_c$  and  $\vec{M}_s$  are the angular momenta of the charged and superfluid components,  $\vec{N}$  is the torque describing their interaction, and  $\vec{K}$  is the external torque acting on the star. In our case, the external torque  $\vec{K}$  is determined by (6). Let us suppose that the magnetic field of the neutron star is related to electric currents in its crust. Therefore,  $\vec{e}_m$  is constant in the reference frame fixed to the charged component. In turn, this means that variations of  $\vec{K}$  in this reference frame are due solely to the slow change in angular-velocity vector  $\vec{\Omega}$  due to the pulsar spin-down, evolution of its inclination angle, and decay of the magnetic field.

For simplicity, we assumed that the superfluid core has a spherical shape, i.e.,  $\vec{M}_s = I_s \vec{\omega}$ . However, generally speaking, the neutron-star crust can have some oblateness along  $\vec{m}$  due to the internal magnetic field (see, e.g., [26]). Therefore, we can write  $\vec{M}_c = I_c \vec{\Omega} + \Delta I \vec{e}_m (\vec{e}_m \cdot \vec{\Omega})$ , where  $I_c + \Delta I$  is the moment of inertia of the charged component along  $\vec{e}_m$  and  $I_c$  the corresponding moment of inertia perpendicular to

$\vec{e}_m$ . Then, neglecting  $\Delta I \vec{e}_m (\vec{e}_m \cdot \dot{\vec{\Omega}}) \ll I_c \dot{\vec{\Omega}}$ , Eq. (24) can be rewritten

$$\begin{aligned} I_c \dot{\vec{\Omega}} &= \vec{K}_{\text{eff}} - \vec{N} \\ &= \vec{K} - \Delta I (\vec{e}_m \cdot \vec{\Omega}) [\vec{\Omega} \times \vec{e}_m] - \vec{N}. \end{aligned} \quad (26)$$

Here, we have introduced the effective torque; in our case, this is

$$\begin{aligned} \vec{K}_{\text{eff}} &= K_0 ((1 - \alpha) \vec{e}_m \cos \chi \\ &\quad - \vec{e}_\Omega + R_{\text{eff}} [\vec{e}_\Omega \times \vec{e}_m]), \end{aligned} \quad (27)$$

where

$$\begin{aligned} R_{\text{eff}} &= R - \frac{\Delta I \Omega^2}{K_0} \cos \chi \\ &= \frac{3}{2} \left( \frac{c}{\Omega r_{ns}} \right) \left( \delta - \frac{\Delta I c^2 r_{ns}}{m^2} \right) \cos \chi. \end{aligned} \quad (28)$$

Then, subtracting (25) from (24), we obtain the following set of equations:

$$\dot{\vec{\Omega}} = \frac{\vec{K}_{\text{eff}}}{I_c} - \frac{\vec{N}}{I_c}, \quad (29)$$

$$\dot{\vec{\mu}} = [\vec{\mu} \times \vec{\Omega}] + \frac{\vec{K}_{\text{eff}}}{I_c} - \frac{\vec{N}}{I_c}, \quad (30)$$

where  $\tilde{I} = I_s I_c / (I_s + I_c)$ .

Let  $\mu \ll \Omega$  at the initial time. Then, in formula (22), in a linear approximation with respect to  $\vec{\mu}$ , we can replace  $\vec{\omega}$  with  $\vec{\Omega}$ ,  $\omega$  with  $\Omega$ , and  $\vec{e}_k$  with  $\vec{e}_\Omega$ . Substituting (22) and (27) into (29) and (30) yields

$$\begin{aligned} \dot{\vec{\Omega}} &= \frac{2\pi}{T_p} [\vec{e}_m \times \vec{\Omega}] \\ &\quad + \frac{1}{\tau_x} [(1 - \alpha(\chi, \varphi_\Omega)) \Omega \cos \chi \vec{e}_m - \vec{\Omega}] \\ &\quad - \frac{\tilde{I}}{I_c} \frac{1}{\tau_r} [(\vec{e}_\Omega \cdot \vec{\mu}) + \vec{\mu}] - \frac{\mathfrak{B}'}{I_c} [\vec{\mu} \times \vec{\Omega}], \\ \dot{\vec{\mu}} &= \left( 1 - \frac{\mathfrak{B}'}{\tilde{I}} \right) [\vec{\mu} \times \vec{\Omega}] + \frac{2\pi}{T_p} [\vec{e}_m \times \vec{\Omega}] \\ &\quad + \frac{1}{\tau_x} [(1 - \alpha(\chi, \varphi_\Omega)) \Omega \cos \chi \vec{e}_m - \vec{\Omega}] \\ &\quad - \frac{1}{\tau_r} [(\vec{e}_\Omega \cdot \vec{\mu}) + \vec{\mu}]. \end{aligned} \quad (31)$$

Here,

$$\tau_x = \frac{I_c \Omega}{K_0} \approx 4.1 \times 10^{15} \text{ s} \left( \frac{P}{1 \text{ s}} \right)^2 \frac{I_{c45}}{B_{12}^2}, \quad (33)$$

$$T_p = \frac{2\pi \tau_x}{R_{\text{eff}}} \approx 3.6 \times 10^{12} \text{ s} \left( \frac{P}{1 \text{ s}} \right) \frac{I_{c45}}{\delta B_{12}^2 \cos \chi}, \quad (34)$$

$$\begin{aligned}\tau_r &= \frac{\tilde{I}}{B\Omega} \approx \frac{2q}{y} \frac{I_c}{I_c + I_s} \left( \frac{P}{1\text{ s}} \right) \\ &\approx (400-8000) \text{ s} \frac{I_c}{I_c + I_s} \left( \frac{P}{1\text{ s}} \right),\end{aligned}\quad (35)$$

where  $I_{c45} = I_c/10^{45} \text{ g cm}^2$  and  $B_{12} = B_0/10^{12} \text{ G}$ . Hence, Eqs. (31), (32) have several dynamic timescales that differ by orders of magnitude. This enable us to considerably simplify them.

Let us first consider the shortest timescale. Since  $\mu \ll \Omega$  at the initial time, the relative change in  $\vec{\Omega}$  during a time  $\tau_r$  is negligible. It is then easy to see from (32) that the timescale of the same order  $\mu$  evolves to  $\mu_{\text{eq}}$  and subsequently remains approximately equal to it. Here,  $\vec{\mu}_{\text{eq}}$  satisfies (32), as well as the condition  $\dot{\vec{\mu}}_{\text{eq}} = 0$  for  $\vec{\Omega} = \text{const}$ . Solving (32) for  $\vec{\mu}$  with a zero left-hand side yields

$$\begin{aligned}\vec{\mu} &\approx \vec{\mu}_{\text{eq}} = \frac{\tau_r}{I_c(\lambda^2\tau_r^2\Omega^2 + 1)} \\ &\times \left[ \vec{K}_{\text{eff}} + \frac{1}{2}(\lambda^2\tau_r^2\Omega^2 - 1) \right. \\ &\left. \times \vec{e}_\Omega(\vec{e}_\Omega \cdot \vec{K}_{\text{eff}}) + \lambda\tau_r\Omega[\vec{K}_{\text{eff}} \times \vec{e}_\Omega] \right],\end{aligned}\quad (36)$$

where  $\lambda = 1 - \mathfrak{B}'/\tilde{I}$ . Substituting (36) into (31) and taking into account that  $\lambda \approx 1$  and  $\tau_r\Omega \gg 1$ , we obtain

$$\begin{aligned}(I_s + I_c)\dot{\vec{\Omega}} &= \left( 1 + \frac{I_s}{I_c} \right) \vec{K}_{\text{eff}} \\ &+ \sigma \frac{I_s}{I_c} \left( 1 + \frac{I_s}{I_c} \right) [\vec{e}_\Omega \times \vec{K}_{\text{eff}}] - \frac{I_s}{I_c} \vec{e}_\Omega(\vec{e}_\Omega \cdot \vec{K}_{\text{eff}}).\end{aligned}\quad (37)$$

This vector equation can be represented as a set of three scalar equations describing the neutron star spin-down, the evolution of the inclination angle, and the precession:

$$\dot{\Omega} = \frac{\Omega}{\tau_x} \frac{I_c}{I_c + I_s} (\sin^2 \chi + \alpha(\chi, \varphi_\Omega) \cos^2 \chi), \quad (38)$$

$$\begin{aligned}\dot{\chi} &= -\frac{\sin \chi \cos \chi}{\tau_x} \\ &\times \left( 1 - \alpha(\chi, \varphi_\Omega) - y \frac{I_s}{I_c} \frac{R_{\text{eff}}}{4\pi q} \right),\end{aligned}\quad (39)$$

$$\dot{\varphi}_\Omega = -\frac{2\pi}{T_p} \left( 1 + \frac{y}{8\pi^2 q} \frac{I_s}{I_c} \frac{1 - \alpha(\chi, \varphi_\Omega)}{R_{\text{eff}} \cos \chi} \right). \quad (40)$$

Note that (38) has precisely the same form as in the rigid-body approximation (cf. [9]). Supposing that  $\dot{\vec{\mu}} \ll \dot{\vec{\Omega}}$  on timescales much longer than  $\tau_r$ , we can eliminate the energy dissipation due to the interaction

of the components. Therefore, introducing the quantity  $\vec{M}_{\text{eff}} = I_c\dot{\vec{\Omega}} + I_s\dot{\vec{\omega}}$ , we can write in the reference frame comoving with the crust:

$$\begin{aligned}\dot{\vec{M}}_{\text{eff}} &= [\vec{\Omega} \times \vec{\mu}] + (I_c + I_s)\dot{\vec{\Omega}} - I_s\dot{\vec{\mu}} \\ &\approx [\vec{\Omega} \times \vec{\mu}] + (I_c + I_s)\dot{\vec{\Omega}}.\end{aligned}\quad (41)$$

On the other hand,  $\dot{\vec{M}}_{\text{eff}} = \vec{K}_{\text{eff}}$ . Thus, the form of the equation for  $\Omega$  does not depend on  $\vec{\mu}$  (the case  $\mu = 0$  corresponds to a rigid-body star). However, it is important here to note that, in spite of the formal coincidence of the equations, generally speaking, the evolution for  $\Omega$  does not coincide with the rigid-body approximation. This is due to the circumstance that the torque  $\vec{K}_{\text{eff}}$  is determined by  $\vec{e}_m$ , whose evolution obviously differs from the case of a rigid-body star.

Furthermore, if the pulsar is not too close to an orthogonal state, the second term on the right-hand side of (40) is negligible compared to the first. Thus,  $T_p$  is the precession period of the star. As we can see from (33) and (34),  $T_p \ll \tau_x$  in this case, where  $\tau_x$  is the timescale for the neutron star spin-down and the evolution of its inclination angle.

Thus, (38) and (39) can be averaged over  $T_p$ , assuming that  $\Omega$  and  $\chi$  vary only weakly over the precession time. Dividing (39) by (38) after this averaging, using the definitions (33) and (34), and neglecting terms of order  $T_p/\tau_x$  yields

$$\begin{aligned}\frac{d\bar{\chi}}{d\bar{P}} &\approx -\frac{1}{\bar{P}} \frac{\sin \bar{\chi} \cos \bar{\chi}}{\sin^2 \bar{\chi} + \bar{\alpha}(\bar{\chi}) \cos^2 \bar{\chi}} \\ &\times \left( 1 + \frac{I_s}{I_c} \right) \left[ 1 - \bar{\alpha}(\bar{\chi}) - y \frac{I_s}{I_c} \frac{R_{\text{eff}}}{4\pi q} \right].\end{aligned}\quad (42)$$

Here,  $\bar{\chi}$  and  $\bar{\Omega}$  are the values of  $\chi$  and  $\Omega$  averaged over the precession period;  $\bar{P} = 2\pi/\bar{\Omega}$ . We also introduced here the function

$$\bar{\alpha}(\chi) = \frac{1}{2\pi} \int_0^{2\pi} \alpha(\chi, \varphi_\Omega) d\varphi_\Omega. \quad (43)$$

The behavior of  $\bar{\alpha}(\chi)$  is shown in Fig. 3. The sharp cutoff of  $\bar{\alpha}(\chi)$  at large inclination angles is due to the appearance and rapid broadening of the range of angles  $\varphi_\Omega$ , within which the outer gap should be realized in the model proposed in Section 3.

Note that, in the absence of oblateness along  $\vec{m}$ , the dependence  $\bar{\chi}(\bar{P})$  (in contrast to  $\bar{\chi}(t)$ ) does not include the magnetic-field intensity; it includes only the ratio of the small-scale to the large-scale field  $\nu$ , which evolves much more slowly (see, e.g., [11]).

It is also necessary to substitute into (42) the expression for  $R_{\text{eff}}$ , which, in turn, includes the parameter  $\Delta I$  describing oblateness of the star. This

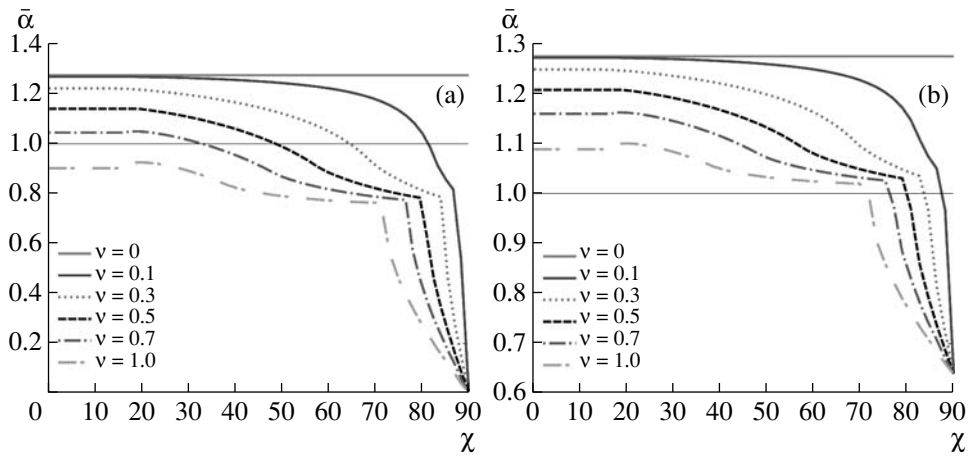


**Fig. 3.** Behavior of the function  $\bar{\alpha}(\chi)$  for various values of the non-dipolarity parameter  $\nu$ : (a) for identical anomalies near both magnetic poles, and (b) for a magnetic anomaly at only one of the poles.

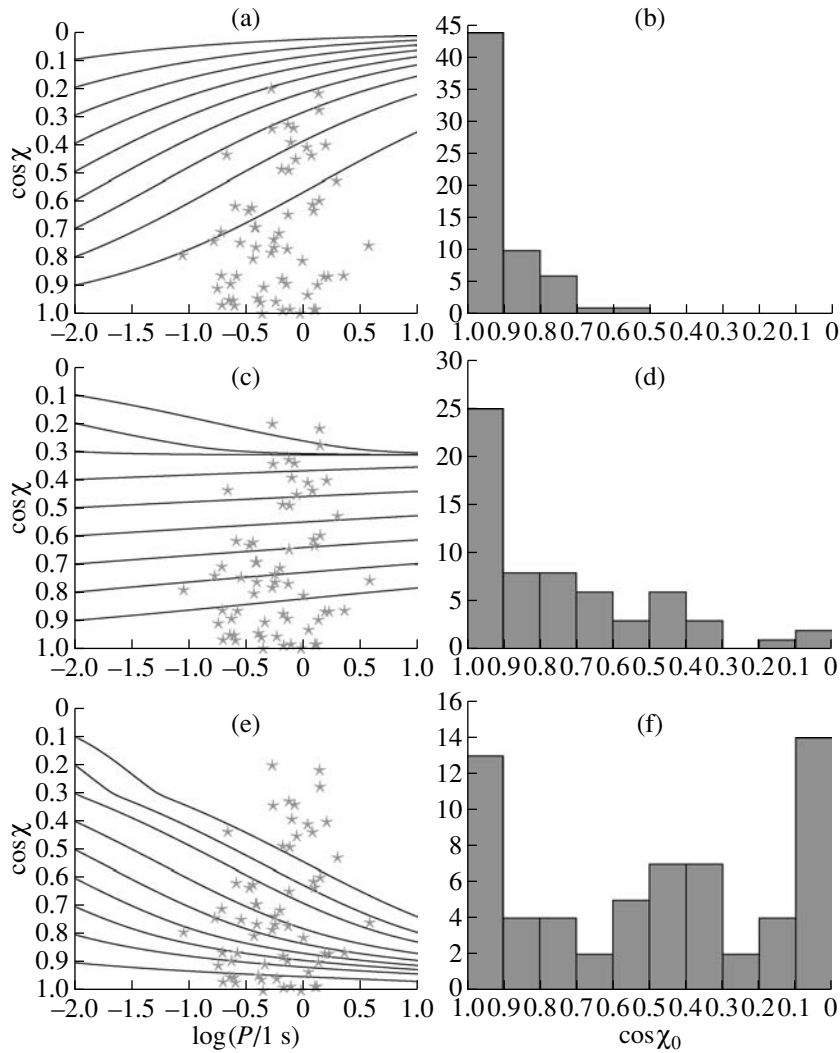


**Fig. 4.** Evolutionary tracks for the case of negligibly small superfluid cores for (a) a dipole field, (c) a magnetic anomaly with  $\nu = 1.0$  at one of the poles, and (e) anomalies with  $\nu = 1.0$  at both poles. The asterisks show the observational date for 62 pulsars from [28]. The histograms (b), (d), and (f) show corresponding distributions of the initial inclination angles assuming that all pulsars are born with an initial period of 10 ms.

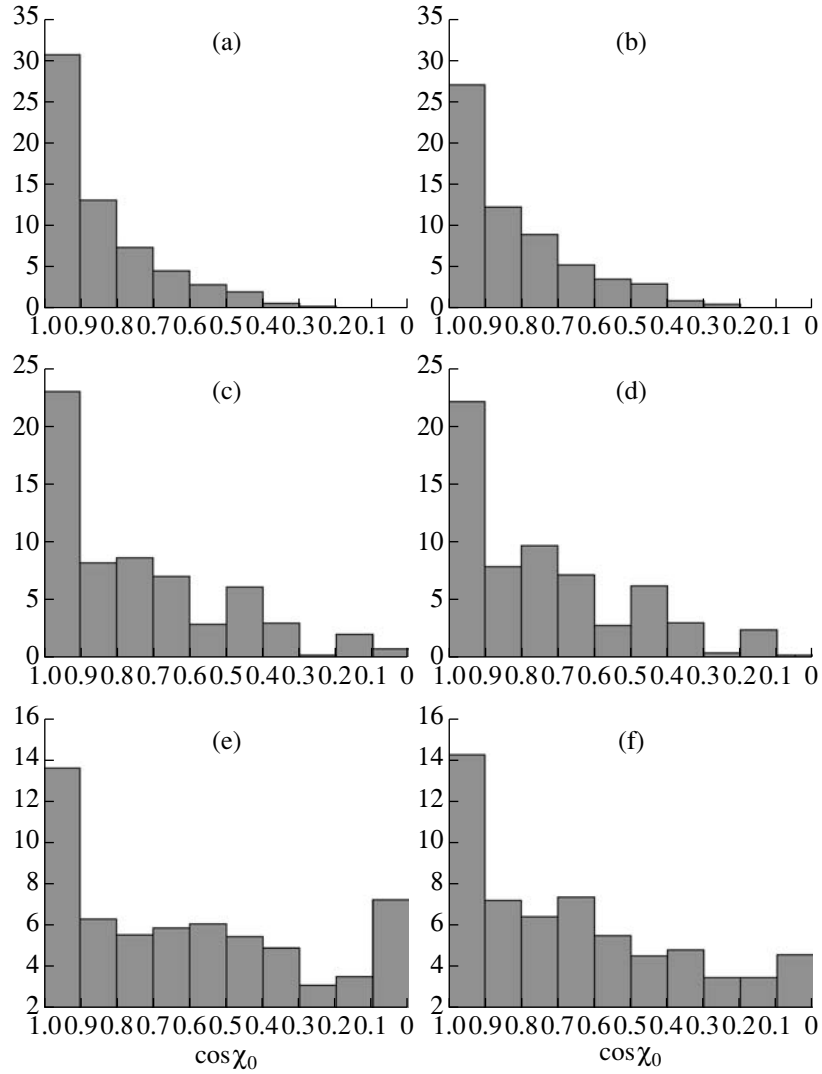


**Fig. 5.** Distribution of the initial inclination angles for the case of (a, b) negligibly small superfluid cores and a dipole field, (c, d) a magnetic anomaly with  $\nu = 1.0$  at one of the poles, and (e, f) anomalies with  $\nu = 1.0$  at both poles. The distributions plotted on the left assume that the probability for a pulsar to be born with initial period  $P_0$  is proportional to  $P_0^{-1}$  in the range from 10 to 300 ms and is zero outside this range, while those on the right assume that this probability is proportional to  $\exp[(P_0 - 100 \text{ ms})^2 / 2(100 \text{ ms})^2]$  for  $P_0 > 10$  ms and is zero otherwise.

parameter can be estimated as [27]

$$\frac{\Delta I}{I_c} \sim \zeta \frac{B_{\text{in}}^2 r_{\text{ns}}^4}{GM_{\text{ns}}}. \quad (44)$$

Here,  $B_{\text{in}}$  is the intensity of the internal magnetic field,  $G$  the gravitational constant, and  $\zeta$  a factor that varies over broad limits in various studies. For instance, the value  $\zeta = 25/8$  was used in [26], while the value  $\zeta = 1/18$  was obtained in [27]. Substituting (28) and (44) together with parameters of a typical neutron star into (42), we finally obtain

$$\frac{d\bar{\chi}}{d\bar{P}} \approx -\frac{1}{\bar{P}} \frac{\sin \bar{\chi} \cos \bar{\chi}}{\sin^2 \bar{\chi} + \bar{\alpha}(\bar{\chi}) \cos^2 \bar{\chi}} \left( 1 + \frac{I_s}{I_c} \right) \quad (45)$$

$$\times \left[ 1 - \bar{\alpha}(\bar{\chi}) - y(\delta - 7\zeta I_{45}) \frac{I_s}{I_c} \frac{9 \times 10^4}{16\pi^2 q} \bar{P} \right].$$

## 6. ANALYSIS AND COMPARISON WITH OBSERVATIONS

If the superfluid core is absent (or is so small that its presence can be neglected), (45) becomes

$$\frac{d\bar{\chi}}{d\bar{P}} = -\frac{1}{\bar{P}} \frac{(1 - \bar{\alpha}(\bar{\chi})) \sin \bar{\chi} \cos \bar{\chi}}{\sin^2 \bar{\chi} + \bar{\alpha}(\bar{\chi}) \sin^2 \bar{\chi}}. \quad (46)$$

As it was shown in [9], the presence of small-scale anomalies of the magnetic field near the magnetic poles results in the pulsar having a stable equilibrium inclination angle given by  $\bar{\alpha}(\chi_{\text{eq}}) = 1$  (Fig. 3).

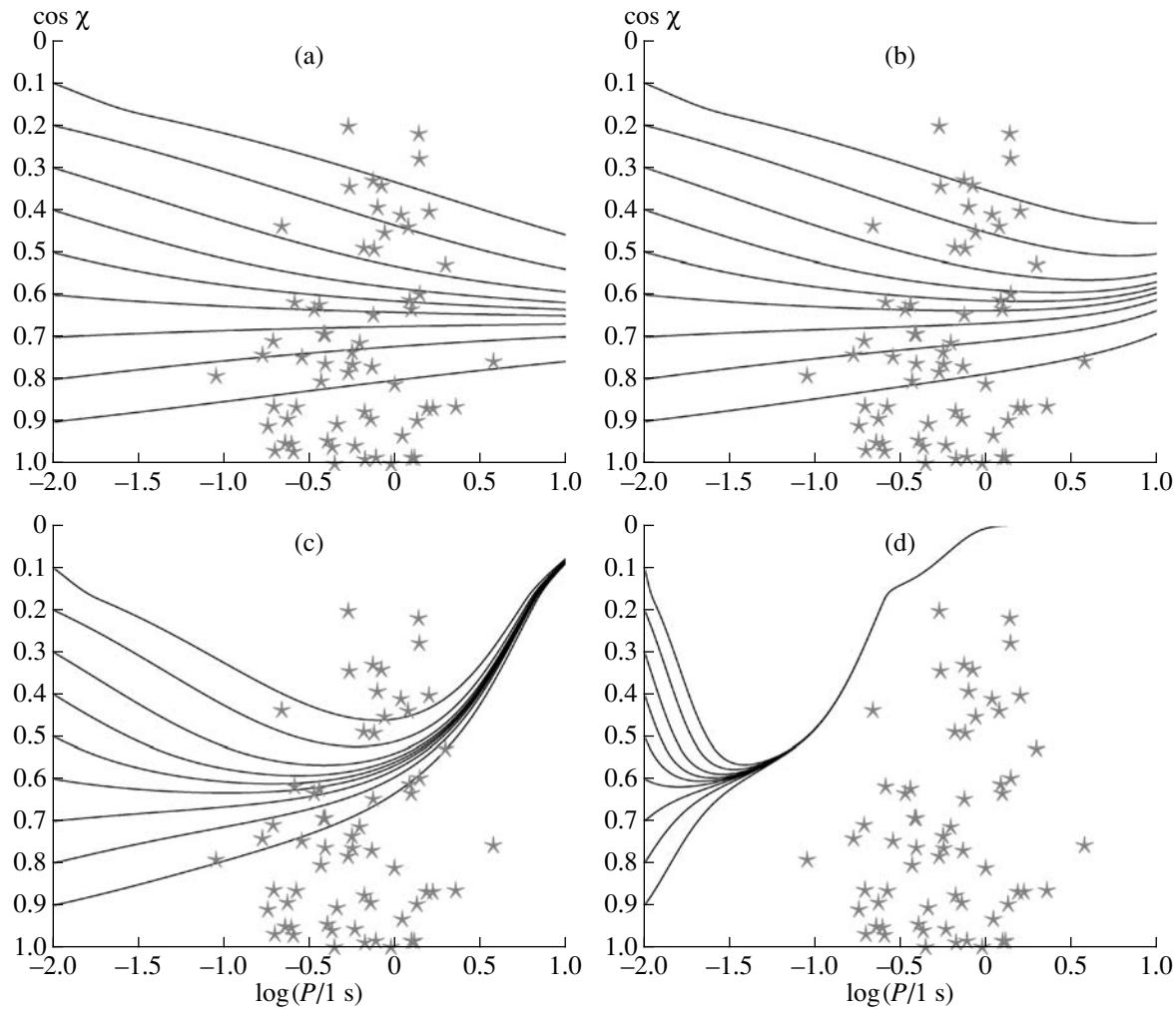


**Fig. 6.** Evolutionary tracks for the case  $\nu = 0.5$ ,  $q = 100$ ,  $\zeta = 0$ , and  $I_s/L_c =$  (a) 0, (b) 0.1, (c) 1, and (d) 10. The observational data are as in Fig. 4.

Let us consider the special case when magnetic anomalies are absent in both poles. In this case,  $\bar{\alpha}(\chi)$  degenerates into a constant,  $\bar{\alpha} = \frac{3}{2}(1 - k) = 1.275$ . Equation (46) can then be integrated:

$$\begin{aligned} \bar{P} &= \bar{P}_0 \left( \frac{\cos \bar{\chi}_0}{\cos \bar{\chi}} \right) \left( \frac{\tan \bar{\chi}}{\tan \bar{\chi}_0} \right)^{\frac{\alpha}{1-\alpha}} \\ &= \bar{P}_0 \left( \frac{\cos \bar{\chi}_0}{\cos \bar{\chi}} \right) \left( \frac{\tan \bar{\chi}}{\tan \bar{\chi}_0} \right)^{-4.64}. \end{aligned} \quad (47)$$

Here,  $\bar{\chi}_0$  and  $\bar{P}_0$  are the initial values of the pulsar inclination angle and period, respectively. Even in this case, the evolution of  $\chi$  is fairly slow. In the absence of magnetic anomalies at the poles, the neutron star tends to approach the orthogonal rotation mode. However, as we can see from (47), a pulsar born with a inclination angle  $\chi$  that is far from  $90^\circ$  will have no time to approach it during its life. In the presence of

magnetic anomalies, the function  $\bar{\alpha}(\chi)$  tends to unity as  $\chi$  approaches  $\chi_{\text{eq}}$ . This means that the evolution of the inclination angle is even slower.

Figures 4a, 4c, and 4e show the evolutionary tracks of pulsars with different initial inclination angles  $\chi$  for the cases of a dipole field, an anomaly at one of the poles, and anomalies at both poles.

If we suppose that all pulsars are born with periods  $\approx 10$  ms, we can estimate the initial inclination-angle distribution of pulsars from the current distribution. We took the data on 62 pulsars from [28], whose inclination angles were measured using data on the maximum of the positional angle derivative, for the current distribution (details of the method are given in [28]). Figures 4b, 4d, and 4f present the initial distributions for the corresponding configurations of the magnetic field. The presence of magnetic anomalies results in a displacement of the initial distribution toward larger inclination angles.

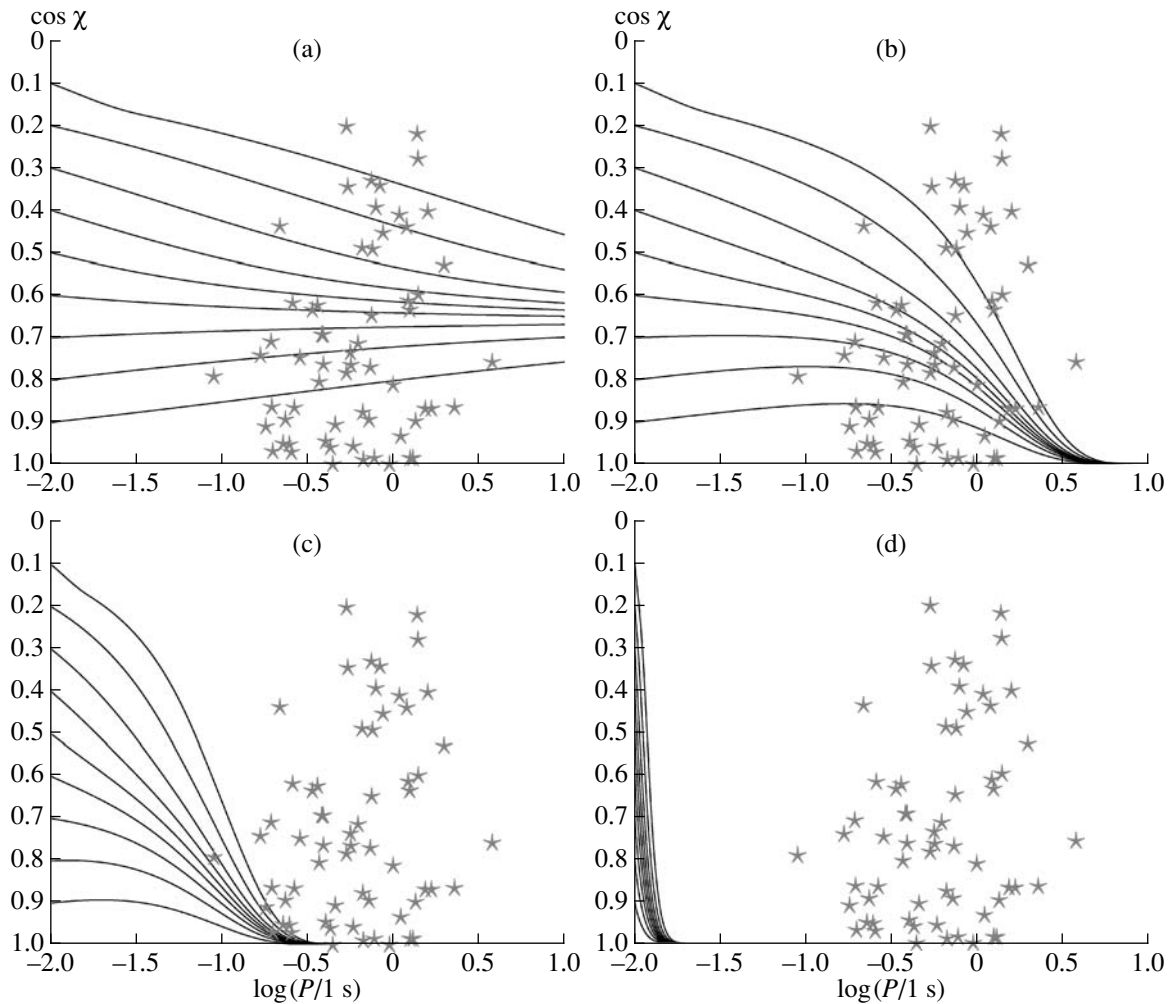


Fig. 7. Same as Fig. 6 for the case  $\zeta = 25/8$ .

However, the observations probably provide evidence [29] that the initial stages of pulsars are distributed fairly smoothly. We used two versions of such distributions: one in which the probability density for each pulsar to be born with initial stage  $P_0$  is proportional to  $P_0^{-1}$  in the range from 10 to 300 ms and is zero outside this range, and another in which this probability density is proportional to  $\exp[-(P_0 - 100 \text{ ms})^2/2(100 \text{ ms})^2]$  at  $P_0 > 10 \text{ ms}$  and is zero otherwise (this latter type of distribution was proposed in [29]). The resulting distributions are shown in Fig. 5.

As we can see from (45), the presence of a superfluid core, first, speeds up the evolution due to the factor  $(1 + I_s/I_c)$  and, second, results in the stable equilibrium inclination angle itself varying with increasing pulsar period. When the oblateness is not very high along  $\vec{m}$ , the equilibrium inclination angle increases, while it decreases in the case of appreciable oblateness. This effect becomes important when the

order of magnitude of the pulsar period reaches

$$P \sim 10^{-4} \text{ s} \frac{I_c}{I_s} \frac{16\pi^2 q}{9y} \frac{1}{|\delta - 7\zeta I_{45}|} \quad (48)$$

$$\approx (0.35-7) \text{ s} \frac{I_c}{I_s} \frac{1}{|\delta - 7\zeta I_{45}|}.$$

Figure 6 presents evolutionary tracks for various ratios  $I_s/I_c$  for the case  $\zeta = 0$ , and Fig. 7 shows the same for the case  $\zeta = 25/8$ . Figure 8 shows the distributions of the initial inclination angles for various ratios  $I_s/I_c$ . These distributions were plotted using the two initial period distributions described above.

## 7. CONCLUSION

We have derived equations describing the spin-down, evolution of the inclination angle, and precession of neutron stars taking into account small-scale surface magnetic fields and superfluid neutrons

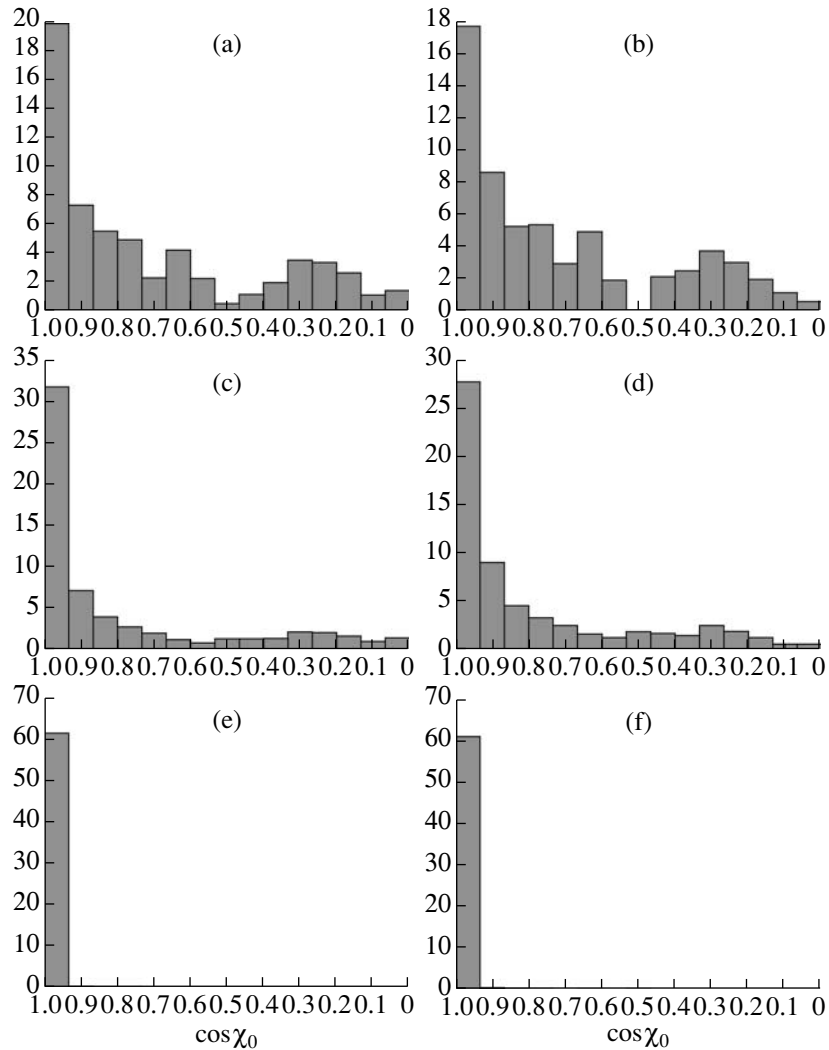


**Fig. 8.** Distributions of the initial inclination angles for the cases  $I_s/I_c = (a, b) 0.1$ ,  $(c, d) 1$ , and  $(e, f) 10$ . The distributions plotted on the left assume that the probability for a pulsar to be born with initial period  $P_0$  is proportional to  $P_0^{-1}$  in the range from 10 to 300 ms and is zero outside this range, while those on the right assume that this probability is proportional to  $\exp[(P_0 - 100 \text{ ms})^2/2(100 \text{ ms})^2]$  for  $P_0 > 10$  ms and is zero otherwise. It was assumed for all the distributions that  $\nu = 0.5$ ,  $\zeta = 0$ , and  $q = 100$ .

in the stellar core. The star was treated as a two-component system, whose components weakly interact via scattering of degenerate electrons of the core on Feynman–Onsager vortices. However, if we assume that the torque describing the interaction of the components is linear in  $\vec{\mu}$ , the most general expression for this torque (in the absence of distinguished directions except for  $\vec{e}_\Omega$ ) is

$$\vec{N} = \mathfrak{A}\vec{\mu} - \mathfrak{A}'[\vec{e}_\Omega \times \vec{\mu}] + \mathfrak{A}''\vec{e}_\Omega(\vec{e}_\Omega \cdot \vec{\mu}). \quad (49)$$

If we use this expression instead of (22) (still assuming weak coupling) we obtain

$$\frac{d\bar{\chi}}{d\bar{P}} \approx -\frac{1}{\bar{P}} \frac{\sin \bar{\chi} \cos \bar{\chi}}{\sin^2 \bar{\chi} + \bar{\alpha}(\bar{\chi}) \cos^2 \bar{\chi}} \quad (50)$$

$$\times \left(1 + \frac{I_s}{I_c}\right) \left[1 - \bar{\alpha}(\bar{\chi}) - \frac{\mathfrak{A}}{I_c \Omega} R_{\text{eff}}\right],$$

which is essentially similar to (42), and therefore yields similar results.

In [9] we considered a neutron star rotating as a rigid body. We found that, in the presence of small-scale surface fields with intensities comparable to that of the dipole field, there should exist a stable equilibrium inclination angle. However, analysis of (46) demonstrates that the rate at which this equilibrium spin tilt is reached is so slow that most pulsars do not have sufficient time to achieve it. In addition, the initial distribution of inclination angles is shifted toward higher values, compared to the distribution for a purely dipole magnetic field.

The presence of neutrons in the superfluid state in the core accelerates the evolution of the inclination angle. In addition, it leads all pulsars to ultimately evolve to either the coaxial or orthogonal state (depending on the degree of oblateness along  $\vec{e}_m$ ). Thus, if not all pulsars are born with inclination angles that are very close to  $0^\circ$  or  $90^\circ$ , we can conclude that the sizes of the superfluid cores probably cannot be very large ( $I_s/I_c \leq 1.0$ ), consistent with the results of the study of the internal structure of neutron stars [30].

We note also that some magnetosphere models assume the presence of only one spin-down mechanism. However, in this case, a pulsar's inclination angle should very quickly reach the region of low losses (near  $0^\circ$  for the magnetodipole mechanism and near  $90^\circ$  for the current mechanism), which does not seem to match the observations (see [31] for details).

#### ACKNOWLEDGMENTS

The authors thank M.E. Gusakov, E.M. Kantor, V.A. Urpin, I.F. Malov, K.A. Postnov, S.B. Popov, and A.Yu. Kirichenko for support and valuable remarks as well as the referee for his or her careful analysis of the article and helpful criticism. This work was supported by the Russian Foundation for Basic Research (project code 10-02-00327) and the Program of State Support of Leading Scientific Schools of the Russian Federation (grant NSh-3769.2010.2).

#### REFERENCES

1. I. F. Malov and E. B. Nikitina, *Astron. Rep.* **55**, 19 (2011).
2. F. Pacini, *Nature* **216**, 567 (1967).
3. V. S. Beskin, *Axisymmetric Stationary Flows in Astrophysics* (Fizmatlit, Moscow, 2005) [in Russian].
4. L. Davis and M. Goldstein, *Astrophys. J. Lett.* **159**, L81 (1970).
5. A. Melatos, *Mon. Not. R. Astron. Soc.* **313**, 217 (2000).
6. P. B. Jones, *Astrophys. J.* **209**, 602 (1976).
7. V. S. Beskin, A. V. Gurevich, and Ya. N. Istomin, *Sov. Phys. JETP* **58**, 235 (1983).
8. R. X. Xu and G. J. Qiao, *Astrophys. J. Lett.* **561**, L85 (2001).
9. D. P. Barsukov, P. I. Polyakova, and A. I. Tsygan, *Astron. Rep.* **53**, 1146 (2009).
10. V. Urpin and J. Gil, *Astron. Astrophys.* **415**, 305 (2004).
11. D. Mitra, S. Konar, and D. Bhattacharya, *Mon. Not. R. Astron. Soc.* **307**, 459 (1999).
12. V. D. Pal'shin and A. I. Tsygan, Preprint FTI Ioffe No. 1718 (Fiz.-Tekh. Inst. im. A.F. Ioffe RAN, St. Petersburg, 1998).
13. E. M. Kantor and A. I. Tsygan, *Astron. Rep.* **47**, 613 (2003).
14. A. G. Muslimov and A. I. Tsygan, *Mon. Not. R. Astron. Soc.* **255**, 61 (1992).
15. Z. Medin and D. Lai, *Mon. Not. R. Astron. Soc.* **382**, 1833 (1997).
16. V. S. Beskin, *Sov. Astron. Lett.* **16**, 286 (1990).
17. S. Shibata, *Mon. Not. R. Astron. Soc.* **287**, 262 (1997).
18. S. Shibata, *Mon. Not. R. Astron. Soc.* **308**, 67 (1999).
19. P. J. Feibelman, *Phys. Rev. D* **4**, 1589 (1971).
20. J. A. Sauls, D. L. Stein, and J. W. Serene, *Phys. Rev. D* **25**, 967 (1982).
21. M. A. Alpar, S. A. Langer, and J. A. Sauls, *Astrophys. J.* **282**, 533 (1984).
22. P. B. Jones, *Mon. Not. R. Astron. Soc.* **371**, 1327 (2006).
23. B. Link, *Astron. Astrophys.* **458**, 881 (2006).
24. I. Easson, *Astrophys. J.* **233**, 711 (1979).
25. T. Sidery and M. A. Alpar, *Mon. Not. R. Astron. Soc.* **400**, 1859 (2009).
26. P. Goldreich, *Astrophys. J. Lett.* **160**, L11 (1970).
27. B. Haskell, L. Samuelsson, K. Glampedakis, and N. Andersson, *Mon. Not. R. Astron. Soc.* **385**, 531 (2007).
28. I. F. Malov, *Radio Pulsars* (Nauka, Moscow, 2004) [in Russian].
29. S. B. Popov and R. Turolla, *Astrophys. Space Sci.* (2012, in press).
30. E. M. Kantor, private commun. (2011).
31. S. A. Eliseeva, S. B. Popov, and V. S. Beskin, arXiv:astro-ph/0611320 (2006).

*Translated by G. Rudnitskii*